PAPER

Check for updates

Study on the influence of inhibitors on the characteristics of coal oxygen composite reactions

Pengjin Liu,[a] Hongwei Mu,[b] Jiafa Du,[a] Xianwei Dong,[c] Jianfei Sun [ID] *[bd] and Yongliang Zhang*[b]

Coal spontaneous combustion fires not only waste coal resources, but also restrict underground safety production. Therefore, research on natural prevention and control of coal fires is particularly important for ensuring coal mine safety production. Based on the theory of coal spontaneous combustion and the mechanism of inhibition, the inhibition performance of sodium hypophosphite inhibitors in the process of coal spontaneous combustion oxidation was studied. Firstly, the CO release and inhibition rates of coal samples and inhibited coal samples during the heating and oxidation process were calculated using a programmed heating method. Then, combined with infrared spectroscopy, the influence of hypophosphite on its surface functional groups during coal spontaneous combustion oxidation was studied from a microscopic perspective. Subsequently, thermogravimetric experiments were conducted to analyze the changes in the thermal characteristic curves of inhibited coal samples at different heating rates and particle sizes. Finally, a kinetic model was proposed to analyze the activation energy of the inhibition reaction. Results indicated that the addition of sodium hypophosphite has a natural inhibitory effect on the oxygen absorption and thermal decomposition stages of coal samples.

1. Introduction

Coal production and usage still rank first in the world, and coalbed methane resources are abundant, which is crucial for coal mine safety requirements.[1] Among them, coal spontaneous combustion fire will not only waste a large number of high-quality coal resources, but also restrict the safety of underground production, bringing hard to estimate losses to the country.[2]

The spontaneous combustion and oxidation of coal is a complex physical and chemical process, and the oxidation rate increases continuously with the oxidation process. It can be roughly divided into three stages: preparation period, natural period, and combustion period.[3] The natural period coal begins to accelerate oxidation, and the combustion period is the most intense stage of coal oxidation. Coal will release different gases at different oxidation stages, manifested macroscopically as varying gas concentrations with temperature. As is well known, the main functional groups that undergo combustion in coal include active groups such as oxygen-containing groups, alkyl

side chains, sulfur-containing groups, and nitrogen-containing groups.[4] Due to the fact that most of the structure of coal contains oxygen-containing functional groups, this component undergoes major losses during the stage of coal oxidation and spontaneous combustion.[5] In addition, clean coal can be pyrolyzed at high temperatures to remove volatiles and prepare coal coke, which can be used as low-impurity amorphous carbon raw materials for the preparation of carbon nano-materials, and undergo nitric acid oxidation to prepare coal-based graphene oxide (GO) materials. At present, coal-based GO materials have potential applications in biosensors, drug delivery systems, energy storage devices, adsorbents, and catalysts.[36,37]

In general, the indicator gases for predicting coal spontaneous combustion are mainly classified into three categories:[6–11] the first category comprises carbon oxides (CO and CO_2). Due to the early appearance of CO gas, it appears in all stages of coal spontaneous combustion, and the release amount shows a strong regularity with temperature increase, which is more common in predicting coal natural fires. The second category comprises saturated hydrocarbons (C_2H_6, C_3H_8, and C_4H_8) and alkane ratios (C_2H_6/CH_4, C_3H_8/CH_4, C_4H_{10}/CH_4, C_3H_8/C_2H_8, and C_4H_{10}/C_2H_8). The amount of gas released is greatly affected by the coal structure, and the detection of such gases during coal spontaneous combustion usually indicates that oxidation has entered an accelerated stage.[12,13] The third category of indicator gas comprises mainly unsaturated hydrocarbons, including C2–C4 olefins and C_2H_2

[a]*Qinghai Shanjin Mining Co., Ltd., Qinghai Haixi, China*

[b]*School of Mechanical and Automotive Engineering, Qingdao University of Technology, Qingdao, China. E-mail: sunjianfei@qut.edu.cn; zhangyongliang@qut.edu.cn; Fax: +86-532-68052755; Tel: +86-532-68052755*

[c]*School of Emergency Management and Safety Engineering, North China University of Science and Technology, Tang Shan, China*

[d]*Key Lab of Industrial Fluid Energy Conservation and Pollution Control (Ministry of Education), Qingdao University of Technology, Qingdao 266520, P. R. China*

alkynes, which are affected by the degree of coal metamorphism and have different critical temperatures during the oxidation and spontaneous combustion process.[14]

At present, flame retardants are widely used in coal mine production fire prevention and extinguishing practices, and have achieved significant results.[15] Moreover, they have the advantages of convenient use and wide application ranges, and are one of the commonly used fire prevention and extinguishing technologies in coal mines at home and abroad. At present, commonly used inhibitors include halogen salt inhibitors ($MgCl_2$, $CaCl_2$, NaCl, sodium hypophosphite, aluminum hypophosphite, *etc.*), ammonium salt inhibitors (NH_4Cl, $(NH_4)_2HPO_5$, *etc.*), ionic liquid inhibitors ([Bmim][OTf], [Bmim][AC], *etc.*), and antioxidant inhibitors (tea polyphenols, citric acid, catechins, *etc.*).[16,17] However, ammonium salt inhibitors are prone to producing harmful gases such as ammonia during use. Ionic liquids and antioxidant inhibitors have good inhibition performance, but their prices are too expensive. Compared to other flame retardants, halogen salt flame retardants are inexpensive, easy to produce, and safe to use. They are widely used in coal mines and have strong water absorption properties. The absorbed water can form a thin film on the surface of the coal, reducing the probability of coal coming into contact with oxygen. They mainly prevent and extinguish fires by exerting their physical flame retardant effect of absorbing water and isolating oxygen, so they are called physical flame retardants.[18-20] The research overview of different inhibitors for suppressing coal spontaneous combustion process is shown in Table 1.

Based on the above-mentioned self-ignition mechanism of coal, the self-ignition conditions of coal can be divided into two categories: physical conditions and chemical conditions. Therefore, the self-ignition inhibition mechanism of coal can also be divided into physical inhibition and chemical inhibition.[21] Physical inhibition mainly aims to prevent coal spontaneous combustion by changing the environmental conditions or physical conditions of the coal itself, so that it does not have the conditions for spontaneous combustion.[22] The inhibition mechanism of chemical inhibitors is to destroy or reduce the active groups in coal molecules with low activation energy that are easily oxidized through chemical action, capture and reduce the free radicals generated during the coal oxidation reaction process, thereby interrupting the chain reaction of coal spontaneous combustion, improving the oxidation reaction

conditions of coal at low temperatures, and making it difficult for coal to achieve spontaneous combustion.[23,24] Usually, physical inhibition is relatively simple, by covering and isolating oxygen to form a membrane film, reducing the probability of coal coming into contact with oxygen, thus achieving fire prevention and extinguishing.[25]

A. C. Smith *et al.*[26] added inorganic salt inhibitors to coal to suppress spontaneous combustion, and the research results showed that sodium nitrate, sodium chloride, and calcium carbonate had the best effect on inhibiting coal spontaneous combustion, while ammonium dihydrogen phosphate, calcium chloride, and ammonium chloride had slightly lower effects. Yukihiro Adachi *et al.*[27] found that mixing amino cationic surfactants and nonionic surfactants in a certain ratio and covering the surface of coal is very effective in preventing coal from heating up. Alkaline inhibitors can effectively reduce the contact between surface active groups of coal and oxygen, and have a good inhibitory effect on coal spontaneous combustion. Acidic inhibitors (such as sodium persulfate, citric acid and other acidic compounds) mainly remove inherent metals from coal, suppress the catalytic effect of some inherent metals on coal spontaneous combustion, and achieve the effect of suppressing coal spontaneous combustion.[28] Previous studies have shown that halogen salt inhibitors have a higher contribution to coal seam inhibition, and further research is needed on the thermal characteristics of coal oxidation inhibition processes.

In this study, the different particle sizes of raw coal samples were first selected, and sodium hypophosphite was chosen as the inhibitor. Different concentrations of inhibitor solutions were added to the raw coal samples to prepare composite coal samples. The coal samples were heated in a temperature oxidation test furnace to analyze the exhaust gas composition of the coal. The chemical structure changes and thermal characteristics of the coal samples before and after oxidation were analyzed to identify the changes in the coal samples before and after oxidation. This study using characterization methods to obtain dynamic monitoring and intelligent warning for suppressing coal oxygen composite reaction and coal spontaneous combustion, as well as active, graded, and collaborative prevention and control of coal spontaneous combustion, and obtain the formation, evolution, and inhibition mechanism of coal spontaneous combustion, and also provide reference and guidance for the development of other types of flame retardants for on-site fire prevention and extinguishing work, as well as

Table 1 Overview of different studies on suppressing the spontaneous combustion process of coal

Coal	Inhibitors	Preparation method	Influence factors	Resistance rate (%)	Ref
Yangquan coal 15 #	30% calcium chloride, 20% sodium silicate	Solvent mixture	Inhibition temperature and solvent concentration	55	31
Dongshan coal	20% ammonium dihydrogen phosphate	—	95–105 °C	88	33
Lignite, gas coal, and fat coal	—	—	3–18% O_2	—	34
Huainan coal	0–10 wt% BMIM BF_4	Impregnation method	0–22% O_2 IL concentration	—	35

theoretical research on fire prevention and extinguishing technology.

2. Experimental section

2.1 Preparation of coal samples and coal resistance samples

The coal sample was removed from the 1184 coal wall of Linan Warehouse in China and transported back to the laboratory. In the actual experiment process, the particle size of middling coal cannot be uniform. The small particle size coal sample has a larger contact area with oxygen, and is more likely to react with oxygen. The oxidation rate is much higher than that of the large particle size coal sample. Therefore, in order to simulate the state of the original coal sample more truly, the mixed particle size of 40–80 mesh was screened in the experiment. The experiment selected sodium hypophosphite as the inhibitor and prepared inhibitor solutions at three concentrations of 15%, 17%, and 20%, respectively. For inorganic flame retardants, solution concentrations ranging from 10% to 20% are usually used. At this concentration, it has a high effect on suppressing coal seam combustion. The relevant operation process can be found in ref. 26–28. First, 100 g of the screened coal sample was mixed with the prepared inhibitor solution in a mass ratio of 4/1, stirred evenly and then left in a dark place for 12 hours before use.

2.2 Elemental analysis and industrial analysis of coal samples

The mixed particle size of 40–80 mesh was selected for elemental analysis and industrial analysis in the experiment. The combination of elemental analysis and industrial analysis of coal can classify the spontaneous combustion tendency and coal type of each coal sample, laying the foundation for subsequent research. Elemental analysis was performed according to the national standard "Coal Sample Collection and Preparation Method" (GB/T476-2008).[29] In the experiment, an Ele-mantar:VarioELcube element analyzer (German) was used to make the coal sample burn and the redox reaction occurred at a specific high temperature, and the resulting oxidation products were then passed through the gas chromatograph to separate various elements in the coal sample. Each group of measurement was carried out three times, and the average value was obtained to reduce the impact of errors. The elemental analysis results of the coal sample are shown in Table 2. C, H, O, and a small amount of N and S are the main elements that make up the coal structure. Among them, the content of C, H, and O

elements accounts for more than 95% of the total organic matter.

The elements and characteristics of different types of coals are different. Industrial analysis of coal can clearly understand the coal quality of various types of coal. The industrial analysis and testing of coal are based on the national standard "Methods for industrial analysis of coal",[30] and the main measurement contents through industrial analysis include moisture, ash content, volatile matter, and fixed carbon, as shown in Table 1. The industrial analysis of spontaneous combustion tendency is divided into three levels: Class I is prone to natural combustion, Class II has a certain tendency towards spontaneous combustion, and Class III is not prone to spontaneous combustion. Based on the results in Table 2, it was classified into Class II. Among them, the ash content of coal is 17.27%, the higher the ash content, the more heat is carried away by the slag, and the lower the utilization rate of coal. The moisture content of raw coal is the highest and the ash content of raw coal is the lowest through experiments. After pre-oxidation treatment, the moisture content of coal decreases, which is conducive to combustion, and the ash content increases, indicating that some organic carbon and water are consumed together.

2.3 Coal spontaneous combustion oxidation experiment

The experiment was conducted mainly using an intelligent coal heating and oxidation test furnace to heat the coal sample. The programmed heating gas chromatography system is mainly divided into two parts: the programmed heating control box and the gas chromatography analyzer. The programmed heating control box is mainly responsible for heating the coal body and collecting tail gas. The gas injection and analysis were performed using a GC-4085 series gas chromatograph developed by the East West Electronic Technology Research Institute in Beijing, China. The data processing system used an A4800 chromatographic data processing workstation. The prepared coal sample was put into an oxidation tank, the natural temperature of the device was adjusted, the heating rate was set to 0.3 °C min^{-1}, and simultaneously compressed air was introduced at a flow rate of 100 mL min^{-1}. During the experiment, the gas was collected once every 5–10 °C temperature rise in the coal sample tank, the collected gas was injected into the gas chromatograph, and the chromatographic workstation was started to analyze and process the data.

2.4 Definition of resistance rate

Different inhibitors and the same inhibitor have significant differences in their inhibition effects in different environments. In practical applications, the inhibition rate is commonly used to measure the effectiveness of inhibition. The inhibition rate refers to the degree to which the inhibitor prevents coal spontaneous combustion, that is, the ratio of the difference in carbon monoxide release before and after the inhibition treatment of the coal sample to the carbon monoxide release before treatment. Its magnitude can be calculated using the following formula:[32]

Table 2 Element analysis and industrial analysis results of coal samples

Number	Name	N%	C%	S%	H%	O%
1 Coal sample	Lin Nancang 1184 Content of each component	1.371	75.91	1.151	4.724	16.844
				Mad%	5.285	
				Vdaf%	38.485	
				Aad%	17.27	
Spontaneous combustion tendency level				II		

$$E = \frac{A - B}{A} \times 100\% \qquad (1)$$

In the formula: E is the resistance rate (%), A is the total amount of carbon monoxide released from the raw coal sample (ppm), and B is the total amount of carbon monoxide released from the coal sample that has been inhibited (ppm). The higher the inhibition rate of the inhibitor, the stronger its ability to prevent coal oxidation.

### 2.5 Fourier transform infrared spectroscopy characterization of functional groups

Before the experiment begins, the coal sample was first pre-treated. Then, 30 g of raw coal sample is divided into two equal parts: one part is added with sodium hypophosphite and the other part is kept as a blank control. The processed coal sample was put into a constant temperature oven and oxidized for 12 hours in a constant temperature drying oven. In order to better understand the effect of the inhibitor on the functional groups on the coal surface, the experiment was conducted at intervals of 10 °C, and coal samples were prepared for each 10 °C increase in temperature, in order to obtain raw coal samples and treated coal samples with different degrees of oxidation. The equipment used in the experiment was a Shimadzu FTIR-8400S Fourier Transform Infrared Spectrometer produced in Japan. The coal sample was mixed with potassium bromide in a ratio of 1/150, vacuum-compressed using a tablet press for 2 minutes, and then placed in the sample chamber of an infrared spectrometer for scanning. The scanning frequency was set to 30 times, and the average value was taken to ensure the smoothness of the infrared spectrum curve. The wavenumber range is from 4600 cm^{-1} to 400 cm^{-1}. Experimental analysis uses changes in absorbance to reflect the changes in functional group concentration, thus achieving quantitative analysis.

2.6 Thermogravimetric analysis of coal resistance characteristics

In coal, there exists a cross-linked bridge structure, and when the temperature reaches a specific requirement of a functional group, the functional group participates in the chemical reaction between coal and oxygen. The temperature at which the functional group participates in the reaction is usually called the characteristic temperature, which can be used to indicate the degree of coal oxidation and spontaneous combustion. The experiment used an STA449F3 comprehensive high-temperature thermogravimetric analyzer produced by the German company Nike, which can simultaneously perform differential scanning calorimetry (DSC). The heating rate of thermogravimetric analysis was 10 °C min^{-1} and 20 °C min^{-1}, and the heating range was between room temperature and 800 °C. The experimental atmosphere used air at a flow rate of 20 mL min^{-1}, and the protective gas used nitrogen with a constant pressure of 0.05 MPa and a constant flow rate of 20 mL min^{-1}.

2.7 Study on oxidation kinetics performance

The oxidation process of coal in air can be roughly represented using the following formula:

$$\text{Oxygen A (g) + coal B (s) = oxidation product C (s)}$$
$$\text{+ generated gas D (s)} \qquad (2)$$
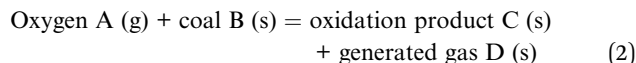
Coal underwent a series of complex chemical reactions when heated and in contact with oxygen, producing oxidation products and some volatile gases. This process was generally considered irreversible. There are two forms of describing dynamics:

Differential form:

$$\frac{d\alpha}{d\alpha} = kf(\alpha) \qquad (3)$$

Integral form:

$$G(\alpha) = kt \qquad (4)$$

In the formula: T is the reaction time (min), α is the conversion rate, *i.e.* the conversion rate of B at time t (%), and k is the reaction rate constant.

It is the mechanism function of oxidation kinetics in differential form. It is the integral form of the dynamic mechanism function, and it is generally believed that the relationship between the rate constant k and the thermodynamic temperature T follows the Arrhenius equation, which states:

$$k = A\exp(-E/RT) \qquad (5)$$

In this equation, A refers to the pre factor, E is the activation energy (kJ mol^{-1-1}), and R is the universal gas constant (8.314 J mol^{-1} K^{-1}).

3. Results and discussion

3.1 Comparison of the performance of inhibitors with different concentrations

The effect of different inhibitors on the oxidation process of coal can be determined by analyzing the concentration of each component. With the change in CO concentration as the evaluation index, the change curve of CO concentration before and after the coal sample resistance at different temperatures is drawn. The curves of CO release and temperature in raw coal samples after adding different concentrations of sodium hypophosphite are shown in Fig. 1.

The results show that the detection time of CO gas in coal samples is basically similar when different concentrations of hypophosphite are added, and it is generally around 50 °C. Before 100 °C, due to the presence of moisture in the coal sample, the CO release of the coal sample with sodium hypophosphite added did not change significantly compared to the original coal sample. After 100 °C, the vaporization of moisture in the coal sample intensified, and the moisture was removed with the airflow. At this time, the temperature difference between the inside and outside of the coal sample tank
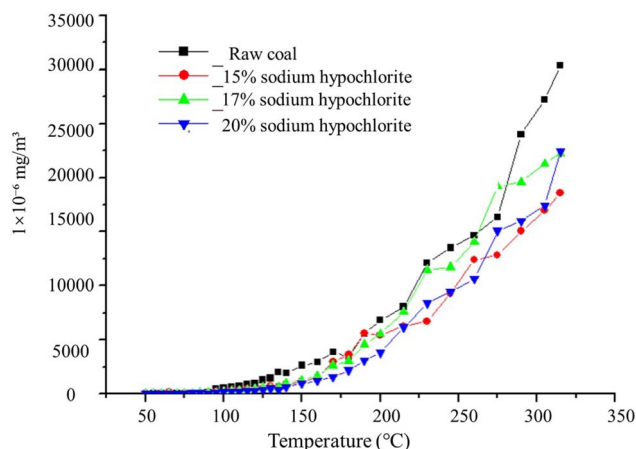
Fig. 1 CO concentration *versus* temperature curve for coal samples with different levels of added sodium hypophosphite.

increased. As the moisture decreased, the CO concentration of the coal sample with added hypophosphite began to decrease compared to the original coal sample, and this is because raising the temperature promoted the volatilization of free water inside the coal, while the inhibitor played a certain role in preventing coal oxidation, thereby reducing the concentration of CO. When the coal oxidation temperature was increased to 300 °C, as the concentration of sodium hypochlorite increased to 17%, the release rate of CO increased. When the concentration of sodium hypochlorite continued to increase to 20%, the release rate of CO decreased. This result indicates that suitable inhibitors under high-temperature conditions are beneficial for the inhibitory effect of hypophosphite on coal samples.

In Fig. 1, it can be seen that the coal sample with 20% concentration of sodium hypophosphite has the lowest CO release, and after 280 °C, the CO release exceeds that of 15% concentration of sodium hypophosphite. Comparing the coal samples with three different concentrations of sodium hypophosphite, the trend of CO release is basically consistent with that of the original coal sample, and it is lower than that of the original coal sample during the heating process. Among them, the best effect is achieved with 20% concentration of sodium hypophosphite.

3.2 Analysis of the inhibition law of sodium hypophosphite on coal oxidation

During the heating process of coal samples, when the temperature reached around 90 °C, the moisture in the coal sample gradually vaporized. At this time, the moisture was removed with the airflow, and the volatilization of moisture carried away a large amount of heat. The temperature of the coal body almost stagnated. As the moisture in the coal body evaporated completely, the temperature difference between the coal sample tank and the programmed heating box intensified. At this time, the temperature of the coal body increased rapidly, and after exceeding 100 °C, the temperature increased in a trapezoidal manner. According to the calculated inhibition rates, as shown

Table 3 Resistance rates of different phosphate concentrations

Inhibitor concentration%	Resistance rate of sodium hypophosphite E/%
15	32.1304
17	17.2003
20	33.1778

in Table 3, when the concentration of sodium hypophosphite was between 15% and 20%, its inhibition rates were 32.1304%, 17.2003%, and 33.1778% at 300 °C, respectively.

As shown in Table 3, the best inhibitory effect is achieved when the concentration of sodium hypophosphite is 20%, mainly because the sodium hypophosphite inhibitor not only has strong moisture absorption and retention properties, but also forms a liquid film on the surface of the coal, greatly reducing the contact area between the coal sample and oxygen, lowering the temperature, and reducing the rate of coal oxidation reaction, achieving the goal of preventing coal oxidation. In the later stage, as the coal temperature rises, the evaporation of water exceeds the limit, and the liquid film formed in the coal body ruptures due to water loss, losing the function of oxygen isolation and inhibition cooling. Sodium hypophosphite also has strong reducibility, which can chemically react with active molecules and free radicals generated by coal at low temperatures, thereby interrupting the free radical reaction chain of coal oxidation reaction and preventing further oxidation and spontaneous combustion of coal.

3.3 Characterization of functional groups for coal oxidation inhibition

3.3.1 Analysis of functional groups in raw coal oxidation characteristics. In order to gain a more intuitive and clear understanding of the changes in the absorption peaks of various functional groups during coal oxidation, infrared experiments were first conducted on coal samples at room temperature. Combined with the characteristic spectra of coal functional group absorption peaks at room temperature, a total of twelve representative characteristic absorption peaks were identified. The absorption peaks were classified according to Fig. 2, and the specific assignments of the absorption peaks are shown in Table 4.

According to Fig. 2 and Table 4, the absorption peaks in the coal sample can be classified into three types: oxygen-containing functional groups, fatty hydrocarbons, and aromatic hydrocarbons. Peaks 4, 8, 11, and 12 in Table 4 belong to oxygen-containing functional groups. Peaks 11 and 12 are caused by the bending and stretching vibrations of free and bound hydroxyl groups in alcohols and phenols, which can be used to determine the presence of alcohols, phenols, and organic acids. The 8th absorption peak belongs to the fatty acid anhydride and is a unique absorption peak in coal, manifested as the stretching vibration of C=O. The C–O vibration of phenols, alcohols, ethers, and esters in coal is manifested as the 4th absorption peak, while the absorbance
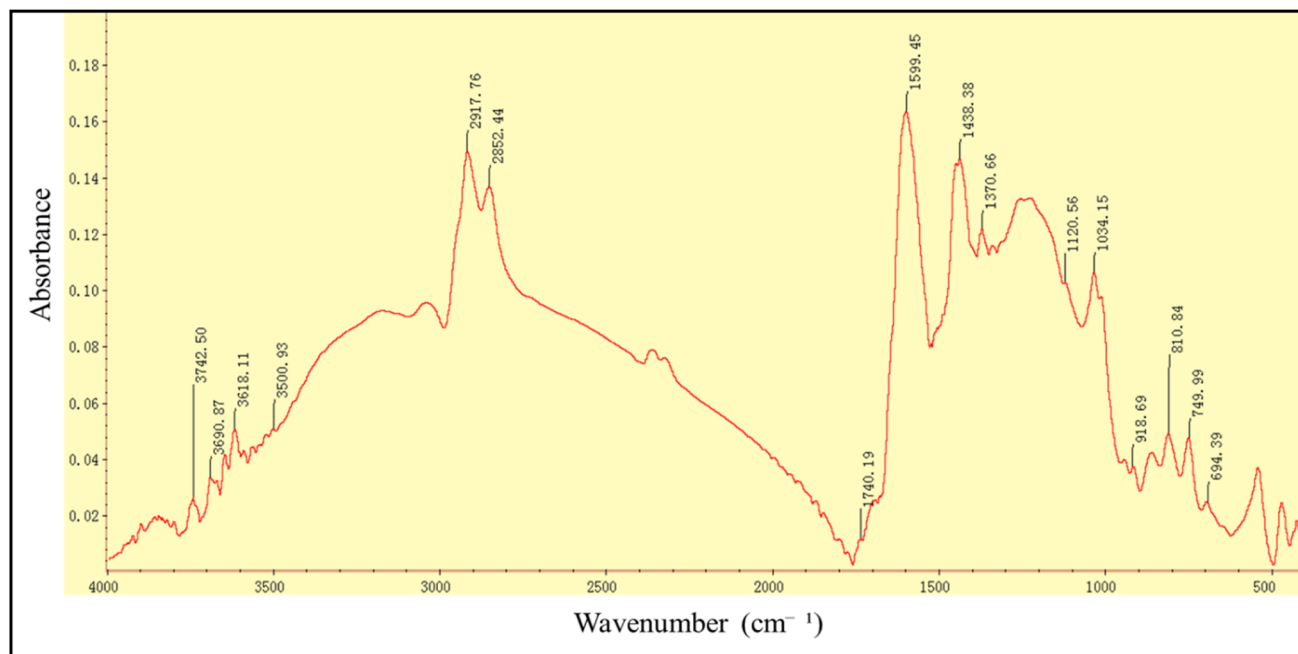
Fig. 2 Fourier transform infrared spectroscopy of coal samples at room temperature.

Table 4 Main coal sample absorption peak of belonging

Spectral peak number	Spectral peak position (cm^{-1})	Corresponding functional groups	Belong
1	694	Out of plane deformation vibration of C–H substituted in benzene ring	Methylene plane vibration
2	810–749	C–H	Out of plane deformation vibration of C–H substituted in benzene ring
3	1034–918	—	Minerals and ash content
4	1120	C–O	C–O of phenols, alcohols, ethers, and esters
5	1370	–CH$_3$	Methyl shear vibration
6	1438	–CH$_2$–	Methylene shear vibration
7	1599	C=C	C=C stretching vibration in aromatic rings
8	1740	C=O	Stretching vibration of fatty acid anhydride C=O
9	2852	–CH$_2$–CH$_3$	Symmetric stretching vibration of methylene and methyl groups
10	2917	–CH$_2$–CH$_3$	Asymmetric stretching vibration of methylene and methyl groups in cyclic or aliphatic compounds
11	3500	–OH	The stretching vibration of OH bound hydroxyl groups
12	3690–3618	–OH	Alcohols, phenols – OH stretching vibration

of absorption peak 4 in the spectrum is only 0.012, indicating a high degree of coal metamorphism and easy oxidation of active functional groups.

Usually, the higher the absorbance of oxygen-containing functional groups in coal, the higher the content. The nature of oxygen-containing functional groups is active, and when they come into contact with oxygen in the air, they are easily attacked by oxygen and oxidized. The bridge bonds in coal molecules break to form unstable peroxides while releasing heat to further promote the decomposition reaction, leading to an increase in coal temperature and the occurrence of coal spontaneous combustion. The higher the degree of coal metamorphism, the lower the content of oxygen-containing functional groups on the coal surface, and the less likely oxidation reactions occur.

The absorption peaks of fatty hydrocarbons are represented by peaks 1, 5, 6, 9, and 10. Peak 10 belongs to the asymmetric stretching of methylene (–CH$_2$) and methyl (–CH$_3$), peak 9 belongs to the symmetric stretching vibration of methylene (–CH$_2$) and methyl (–CH$_3$), peak 6 belongs to the shear vibration of methylene (–CH$_2$), peak 5 is the shear vibration of methyl (–CH$_3$), and peak 1 is generated by the planar vibration of methylene.

Peaks 2 and 7 belong to the category of aromatic hydrocarbons, and the stretching vibration of the C=C double bond in

the skeleton structure of mononuclear aromatic hydrocarbons is shown as peak 7 in the spectrum. The absorption peak 2 comes from the deformation vibration of the C–H bond on the surface of aromatic hydrocarbons, and peak 3 does not correspond to any functional groups and belongs to minerals. Its absorbance is 0.016, indicating that the mineral content is not very high, that is, the ash content of kaolinite minerals and sulfur-containing substances in the coal sample is relatively low.

3.3.2 Analysis of the characteristic functional groups for inhibiting coal oxidation at different temperatures.

The functional groups in coal molecules undergo a series of complex chemical reactions during the oxidation heating process due to the dual effects of oxygen and inhibitors. At this time, the changes in functional groups are mainly manifested as changes in the intensity and number of absorption peaks. Due to the constant vibration frequency of specific functional groups, *i.e.* the position of the absorption peak, the effect of the inhibitor on a certain functional group in coal molecules can be obtained by observing the changes in the intensity of the absorption peak of specific functional groups in the raw coal sample and the coal sample after inhibition at different oxidation stages, and thus the inhibition law of the inhibitor on the coal sample can be obtained.

The comparison results of characteristic functional groups between the raw coal sample and the deactivated coal sample after constant temperature oxidation at 90–300 °C are shown in Fig. 3 and 4. For oxygen-containing functional groups, the peaks 11 and 12 attributed to –OH were significantly enhanced in the coal sample treated with inhibition at 90 °C compared to the original coal sample. The absorbance of the coal sample with added sodium hypophosphite increased by about two times, mainly due to the hydrophilicity of hypophosphite. During the low-temperature stage, hypophosphite absorbs water from the surrounding environment, and water molecules are polar molecules with larger dipole moment vibration amplitudes. Therefore, the intensity of the –OH spectrum peak was enhanced, and sodium hypophosphite exhibited a stronger intensity due to its presence of crystalline water. As the temperature increased to 300 °C, the absorption rate of water by hypophosphite became lower than the evaporation rate, and the water content began to decrease. At the same time, some highly active hydroxyl groups detach from the coal body and generate water after heating. Therefore, the intensity of the –OH spectrum peak gradually approaches consistency with the original coal sample as the temperature increased.

The peak intensity of peak 8 in the raw coal sample gradually increased with temperature, and the absorbance degree
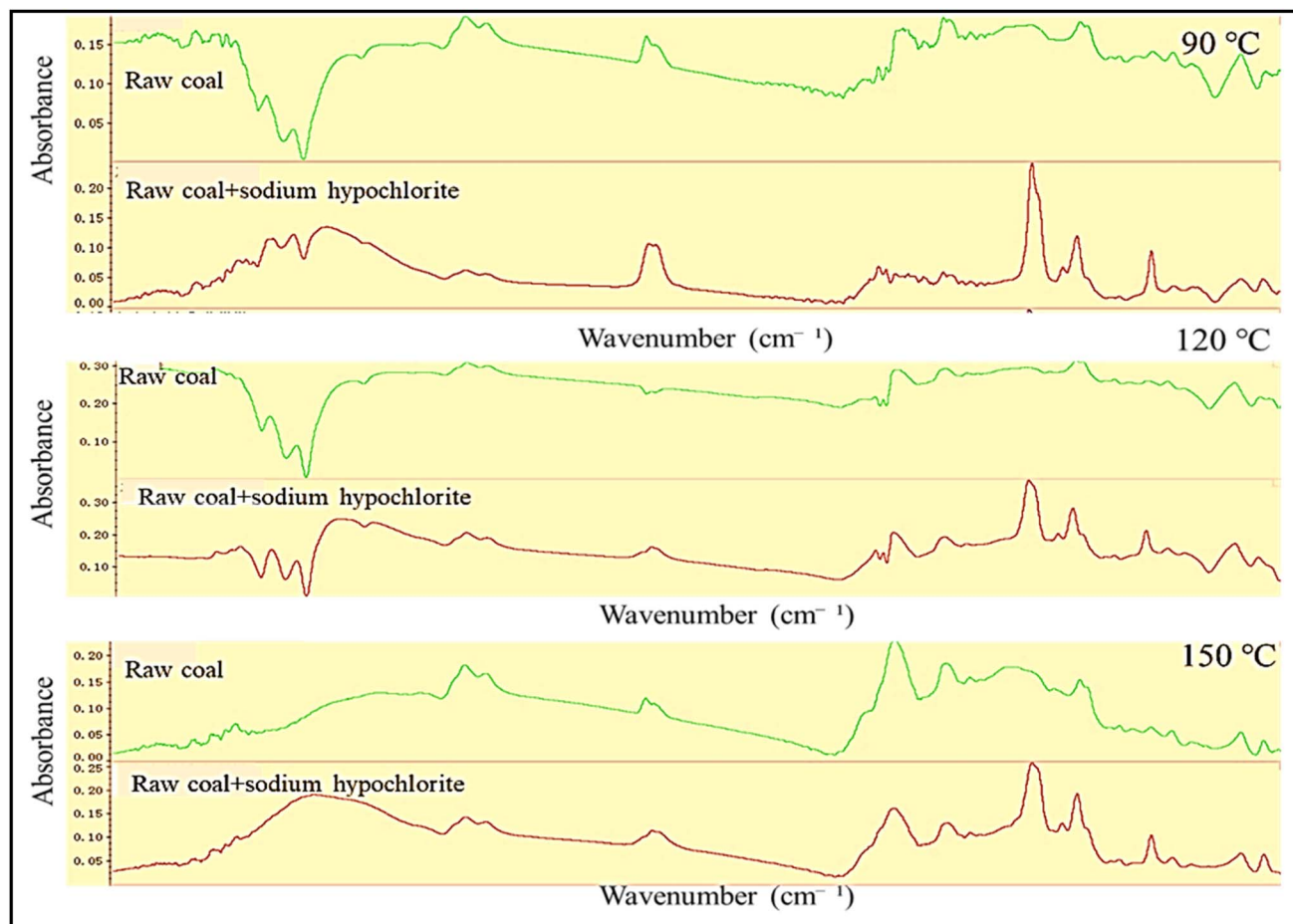

Fig. 3 Fourier transform infrared spectra of coal sample oxidation in the low temperature range: 90 °C, 120 °C, and 150 °C.
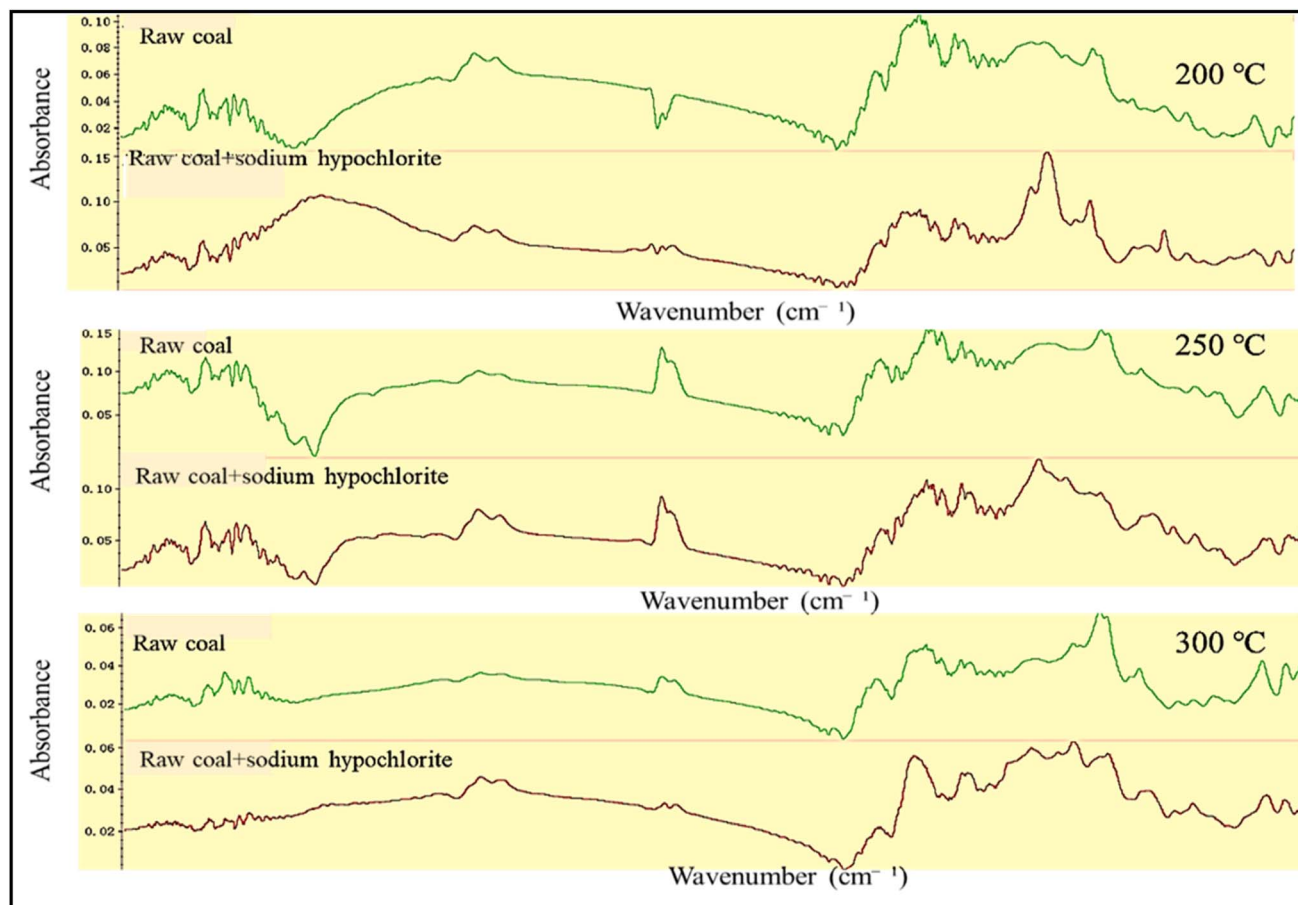
Fig. 4 Fourier transform infrared spectra of coal sample oxidation in the high temperature range: 200 °C, 250 °C, and 300 °C.

increased from 0.016 at 90 °C to 0.138 at 300 °C, indicating that more functional groups decompose to form C=O. After adding sodium hypophosphite, the absorbance of C=O decreased. The reason may be that at high temperatures, sodium hypophosphite decomposes to produce hypophosphite ions, which have strong reducibility, resulting in a decrease in the peak intensity of some carbonyl groups in coal molecules.

Peak 4 belongs to C–O of phenols, alcohols, ethers, and esters, and the absorbance shows a trend of first increasing and then decreasing. At 150 °C, the absorbance reaches its maximum value of 0.322, indicating that some functional groups undergo cleavage to produce C–O. After adding sodium hypophosphite, peak 4 shows a similar trend to the original coal sample, and there is not much difference in C–O absorbance, indicating that the inhibitory effect of sodium hypophosphite on C–O bonds is not significant.

Peaks 5, 6, 9, and 10 belong to fatty hydrocarbons, mainly the stretching vibration of methyl and methylene groups. The spectral peak intensity in the raw coal sample is relatively low, and it shows a decreasing trend with increasing temperature, indicating that these functional groups easily undergo oxidation–reduction. After adding sodium hypophosphite, the intensity of spectral peaks in the coal sample decreased, with

peaks 9 and 10, showing the most obvious. This is mainly due to the decomposition of hypophosphite, which prevents the oxidation process of methyl and methylene groups.

Peak 7 comes from the skeletal vibration of C=C in the aromatic nucleus. With the increase in temperature of the raw coal sample, the absorbance of C–H in the periphery of aromatic hydrocarbons changes significantly, which may be due to the small bond energy of C–H, which is not strong and easy to break. After adding sodium hypophosphite, sodium hypophosphite gradually electrolyzes with the increase in temperature to produce hypophosphite ions, which take over the position of H in C–H of the benzene ring periphery and maintain the relatively stable structure of the benzene ring.
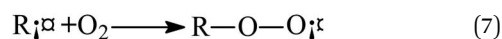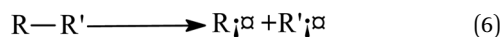
Peak 3 attributed to minerals has remained stable, with no significant difference in peak intensity between the original coal sample and the blocked coal sample.

3.3.3 Analysis of coal oxidation characteristic peaks at different temperatures. In infrared spectroscopy, the peak area is directly proportional to the content of the corresponding substance. By fitting the overlapped peaks in a specific frequency band in the infrared spectrum and calculating the peak area of the separated individual peak, the functional group content can be qualitatively analyzed. Taking into account the difficulty of oxidation of functional groups on the coal surface,

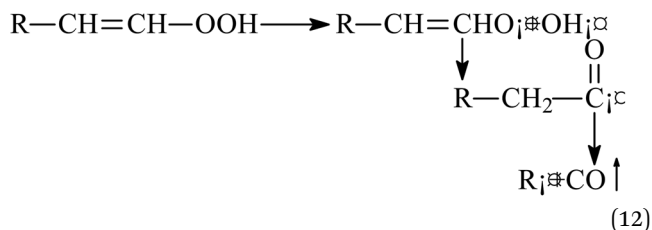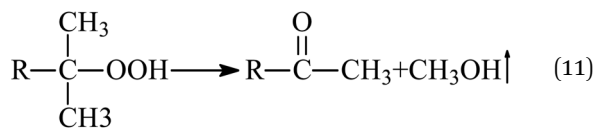the main analysis objects are oxygen-containing functional groups and fatty groups.
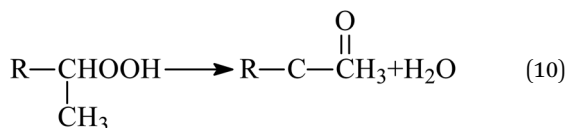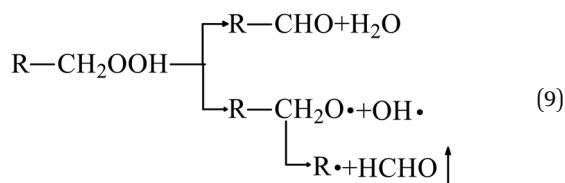
In general, the low-temperature oxidation reaction of coal mainly goes through the following processes:[32,38]

(i) Coal is damaged by external forces, generating a large amount of free radicals that react with oxygen in the air, as shown in the following reaction equation:

$$R{-}R' \longrightarrow R{\cdot} + R'{\cdot} \qquad (6)$$

$$R{\cdot} + O_2 \longrightarrow R{-}O{-}O{\cdot} \qquad (7)$$

$$R{-}O{-}O{\cdot} + R'H \longrightarrow R{-}O{-}O{-}H + R'{\cdot} \qquad (8)$$

In the reaction equation, R is the alkyl group, R˙ – with electronic functional groups and ˙ – unpaired electrons.

(ii) The oxidation reaction of free radicals is an exothermic reaction, providing conditions for further reaction of peroxide free radicals. Different free radical peroxides have different reactions, as shown in the following reaction equation:

$$R{-}CH_2OOH \longrightarrow \begin{cases} R{-}CHO + H_2O \\ R{-}CH_2O{\cdot} + OH{\cdot} \\ \quad \hookrightarrow R{\cdot} + HCHO\uparrow \end{cases} \qquad (9)$$

$$\underset{\underset{CH_3}{|}}{R{-}CHOOH} \longrightarrow R{-}\overset{\overset{O}{\|}}{C}{-}CH_3 + H_2O \qquad (10)$$

$$\underset{\underset{CH3}{|}}{\overset{\overset{CH_3}{|}}{R{-}C{-}OOH}} \longrightarrow R{-}\overset{\overset{O}{\|}}{C}{-}CH_3 + CH_3OH\uparrow \qquad (11)$$

$$R{-}CH{=}CH{-}OOH \longrightarrow R{-}CH{=}CHO{\cdot} + OH{\cdot}$$
$$\downarrow$$
$$R{-}CH_2{-}\overset{\overset{O}{\|}}{C}{\cdot}$$
$$\downarrow$$
$$R{\cdot} + CO\uparrow \qquad (12)$$

(iii) As the free radical peroxide reaction proceeds, CO_2 gas is generated, as shown in the following reaction equation:

$$R{-}\overset{\overset{O}{\|}}{C}{-}O{\cdot} \longrightarrow R{\cdot} + CO_2\uparrow \qquad (13)$$
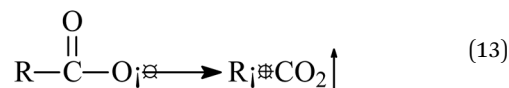
Fig. 5 shows the relationship curve between the absorption peak area intensity of oxygen-containing functional groups (–C–O) and fatty hydrocarbons (RCH_3 and R_2CH_2) after peak fitting and temperature changes.

The content of RCH_3 groups in the raw coal sample began to increase with the increase in temperature and showed a decreasing trend after 150 °C. After adding sodium
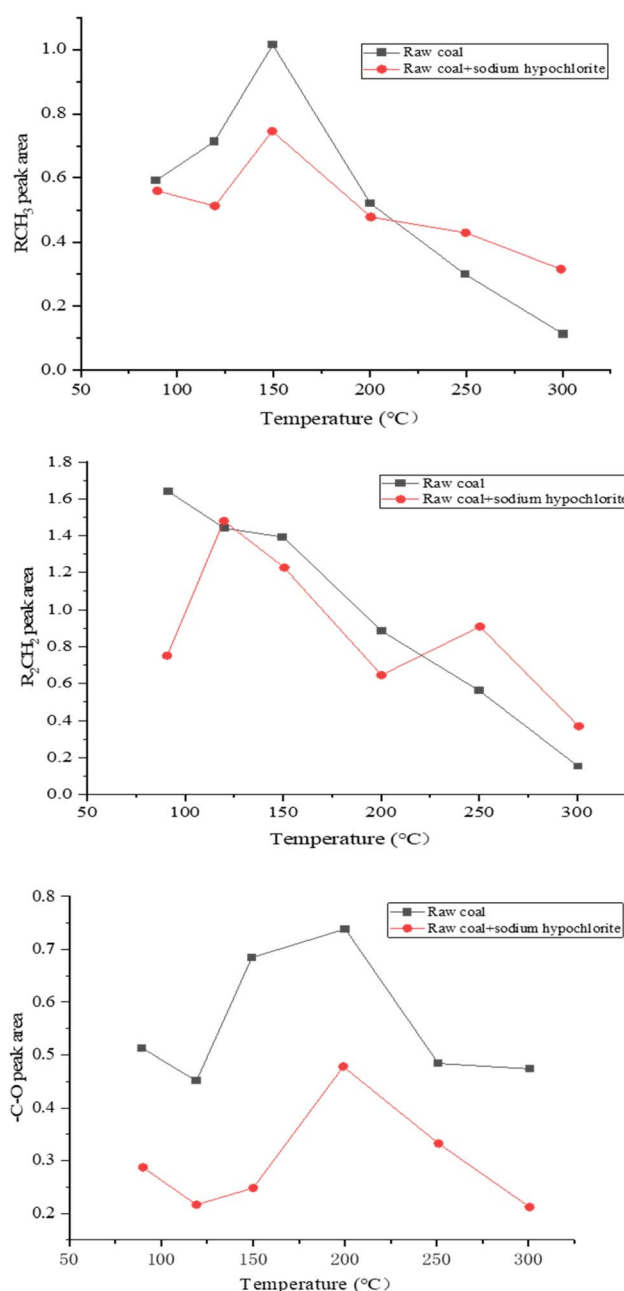

Fig. 5 Changing curve of peak absorption area of RCH_3 and R_2CH_2 and −C−O group and temperature.

Paper

hypophosphite, the content of RCH$_3$ groups in the coal sample decreased to a certain extent. After 150 °C, the content of RCH$_3$ groups in the coal sample with sodium hypophosphite added was similar to that of the original coal sample, but lower than that of the original coal sample. After 220 °C, the content of RCH$_3$ groups in the coal sample with sodium hypophosphite added exceeded that of the original coal sample, indicating that the inhibitory effect of sodium hypophosphite on RCH$_3$ groups has ended.

The content of R$_2$CH$_2$ groups in raw coal samples decreases with the increase in temperature, while the content of R$_2$CH$_2$ groups in coal samples with sodium hypophosphite added between 90 °C and 120 °C increases and is lower than that in raw coal samples. As the temperature increases, the difference in the R$_2$CH$_2$ group content between coal samples with added sodium hypophosphite and raw coal gradually decreases, indicating that the inhibitory effect of sodium hypophosphite on the R$_2$CH$_2$ group content gradually weakens with the increase in temperature. When the temperature approaches 250 °C, the R$_2$CH$_2$ group content of coal samples with added sodium hypophosphite exceeds that of raw coal samples, and the inhibitory effect of sodium hypophosphite on R$_2$CH$_2$ groups ends.

The content of –C–O in the raw coal sample shows an approximate trend of first increasing and then decreasing with the increase in temperature, reaching its peak at around 200 °C. After adding sodium hypophosphite, the content of –C–O in the coal sample shows a similar trend of change. At 150–200 °C, sodium hypophosphite is added to the coal sample. The content of C–O significantly decreased, and sodium hypophosphite had a certain inhibitory effect on C–O throughout the entire heating process.

3.4 Thermogravimetric analysis of thermal characteristics of coal oxidation inhibition

The structure and composition of coal are different, and through thermogravimetric analysis of the characteristic temperatures of raw coal and coal inhibition samples, the higher the characteristic temperature point, the more demanding the conditions required for oxidation reaction, and the less likely the oxidation reaction is to occur. On the contrary, the lower the characteristic temperature point, the more favorable it is for the oxidation reaction to proceed.

The TG-DTG-DSC curve of the raw coal sample is shown in Fig. 6, and the corresponding characteristic temperature points of the coal sample are shown in Table 5. In the initial stage, as the temperature increases, the TG curve shows a slight but not very obvious increase, which ends at 43.2 °C. During this stage, the coal sample is mainly subjected to physical adsorption, and the increase in temperature increases the internal energy of the coal, accelerating the physical desorption process. Chemistry gradually dominates, and the pre-existing gases and gases produced by chemical reactions in the coal escape, resulting in a decrease in the weight of the coal. When the temperature increases to 59.1 °C, the lowest point appears on the DTG curve, which is the point of maximum weight loss rate. When the
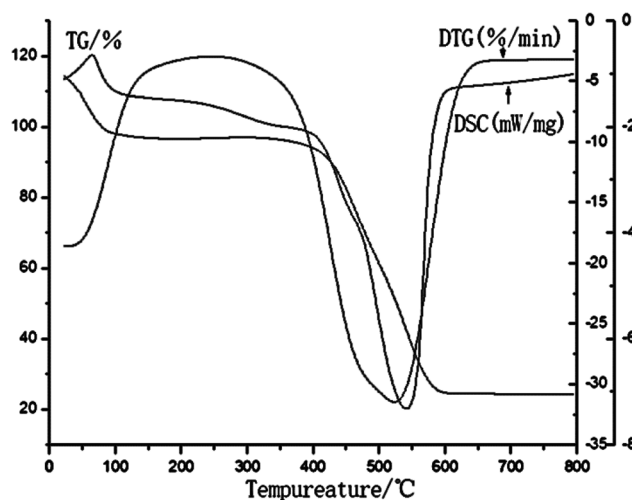

Fig. 6 Raw coal sample thermal analysis curves.

temperature increases to 191.2 °C, due to the high temperature, the amount of oxygen absorbed by the coal increases sharply. When the temperature reaches 206.3 °C, the cracking of large molecules in coal molecules accelerates, and the active groups require more oxygen. The oxygen adsorption rate reaches its maximum. When the coal temperature reaches 430.5 °C, the internal energy between coal molecules reaches the bond energy for breaking the benzene and aromatic ring structures, making it difficult to oxidize and break the relatively stable cyclic molecules in the low-temperature stage. The reaction between coal and oxygen is most intense at 480.8 °C. After 570.7 °C, the TG curve gradually slows down, indicating that the organic compounds composed of carbon, hydrogen, *etc.* in coal molecules are completely burned.

Within the temperature range of 43.2–570.7 °C, sodium hypochlorite covers the surface of coal, preventing contact between coal and oxygen, thereby inhibiting the coal oxygen reaction. When the amount of flame retardant additives increases, the quality loss increases, even exceeding the quality loss of raw coal.[39] When the temperature exceeds 430.5 °C, the coal sample enters the rapid combustion stage, leading to the decomposition and formation of gaseous products. The formation of gaseous products may dilute the oxygen concentration on the coal surface.[40] Continuing to increase the temperature, when the temperature exceeds the decomposition temperature of the flame retardant, a small amount of heat energy will be released, and the mass loss will slightly increase. In addition, the released gas dilutes the oxygen concentration.[41,42]

Table 5 Characteristic temperature of the original coal sample[a]

T_1/°C	T_2/°C	T_3/°C	T_4/°C	T_5/°C	T_6/°C	T_7/°C
43.2	59.1	191.2	226.3	430.5	520.8	570.7

[a] T_1: high adsorption temperature; T_2: critical temperature; T_3: dry cracking temperature; T_4: growth rate temperature; T_5: ignition temperature; T_6: maximum weight loss rate temperature; T_7: Burning temperature.

3.4.1 Influence of heating rate on coal oxidation resistance characteristics. In Fig. 7(a), 1 and 3 show the TG and DTG curves of coal samples with added sodium hypophosphite at 10 °C min⁻¹, respectively, 2 and 4 show the TG and DTG curves of coal samples with added sodium hypophosphite at 20 °C min⁻¹. In Fig. 7(b), 1 and 3 show the DSC and DDSC curves of the raw coal sample at 10 °C min⁻¹, respectively, 2 and 4 show the DSC and DDSC curves of the coal sample with added sodium hypophosphite at 20 °C min⁻¹. The difference in thermal characteristic values between the raw coal sample and the deactivated coal sample can be determined through the thermal characteristic curves at different heating rates, as shown in Table 6.

According to Fig. 7 and Table 6, it can be seen that different heating rates have a significant impact on the oxidation process of coal samples. After changing the heating rate, both the raw coal sample and the blocked coal sample show varying degrees of backward shift in the TG curve. When adding sodium hypophosphite to the coal sample, the maximum heat loss of the coal sample at a heating rate of 10 °C min⁻¹ was basically the same as that of the original coal sample. However, the maximum heat loss at a heating rate of 20 °C min⁻¹ decreased significantly. The maximum heat loss difference between the original coal sample at a heating rate of 10 °C min⁻¹ and 20 °
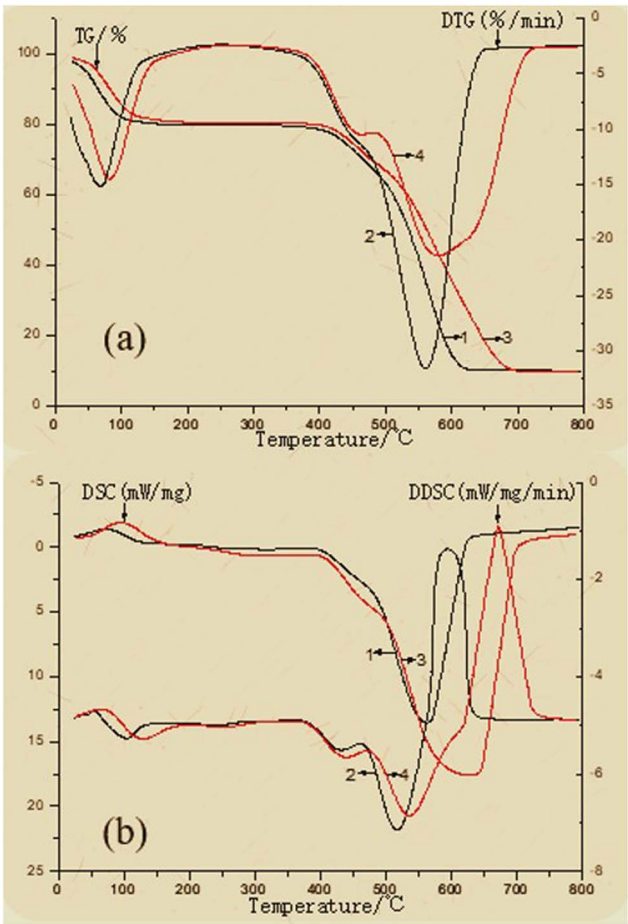

Fig. 7 Thermal analysis of coal samples with added sodium hypophosphite: (a) TG-DTG; (b) DSC-DDSC.

Table 6 Thermal characteristics at different heating rate values

Sample	Heating rate/(°C min⁻¹)	Weight gain range/°C	Range of weightlessness/°C	Maximum weight loss/°C	Maximum weightlessness rate/(%/min)	Maximum hot spot/°C	Maximum heat loss/(mW mg⁻¹)
Raw coal	10	194–291	195–610	520	3.7863	543.29	14.28
	20	217–305	209–675	597	5.896	608	22.26
Add sodium hypophosphite coal sample	10	224–279	213–680	593	6.858	569.52	14.01
	20	242–288	234–693	580	3.7804	635.67	17.74

Sample	Particle size/mesh	Weight gain range/°C	Weight loss range/°C	Maximum weight loss point/°C	Maximum weight loss rate/(%/min)	Maximum heat release point/°C	Maximum heat loss/(mW mg⁻¹)
Raw coal	40–80	194–291	291–610	520	3.7863	543.29	14.28
	150–200	156–287	287–688	458	5.4578	456.83	14.59
Add sodium hypophosphite coal sample	40–80	224–279	279–680	593	6.858	569.52	14.01
	150–200	174–290	290–692	493	7.821	498.51	18.29

C min^{-1} was 7.98 mW mg^{-1}. After adding sodium hypophosphite, the maximum heat loss difference of the coal sample at different heating rates was 3.71 mW mg^{-1}.

3.4.2 Influence of different particle sizes on the oxidation inhibition characteristics of coal. Considering the influence of particle size on the experiment, the heating rate was set at 10 °C min^{-1}, and coal samples with mixed particle sizes of 150–200 mesh were selected for experimental comparison. All other experimental conditions were kept consistent. The influence of particle size on thermal characteristic values during coal oxidation and inhibition can be obtained from the thermal characteristic curves of raw coal samples and inhibition coal samples at different particle sizes. In Fig. 8(a), 1 and 3 represent the TG curve and DTG curve of coal samples with a particle size of 40–80 mesh, 2 and 4 represent the TG curve and DTG curve of coal samples with a particle size of 150–200 mesh, respectively. In Fig. 8(b), 1 and 2 represent the DSC curve and DDSC curve of coal samples with a particle size of 40–80 mesh, and 2 and 4 represent the DSC curve and DDSC curve of coal samples with a particle size of 150–200 mesh, respectively.

In Fig. 8(a), 1 and 3 represent the TG curve and DTG curve of coal samples with a particle size of 40–80 mesh, and 2 and 4 represent the TG curve and DTG curve of coal samples with a particle size of 150–200 mesh, respectively. In Fig. 8(b), 1 and 2 represent the DSC curve and DDSC curve of coal samples with a particle size of 40–80 mesh, and 2 and 4 represent the DSC curve and DDSC curve of coal samples with a particle size of 150–200 mesh, respectively.

Fig. 8(c) and (d) intuitively reflect the trend of particle size variation with temperature. At the same heating rate, as the particle size increases, the thermal characteristic curves of both the raw coal sample and the coal sample with added hypophosphite shift backward, and the weight gain range decreases while the weight loss range expands. Under the same particle size, the maximum weight loss rate of coal samples with added sodium hypophosphite changed most significantly. With the increase in particle size, the maximum weight loss point in the raw coal sample shifted backward by 62 °C, and the maximum heat release point shifted backward by 86.46 °C. Compared with the same conditions of 150–200
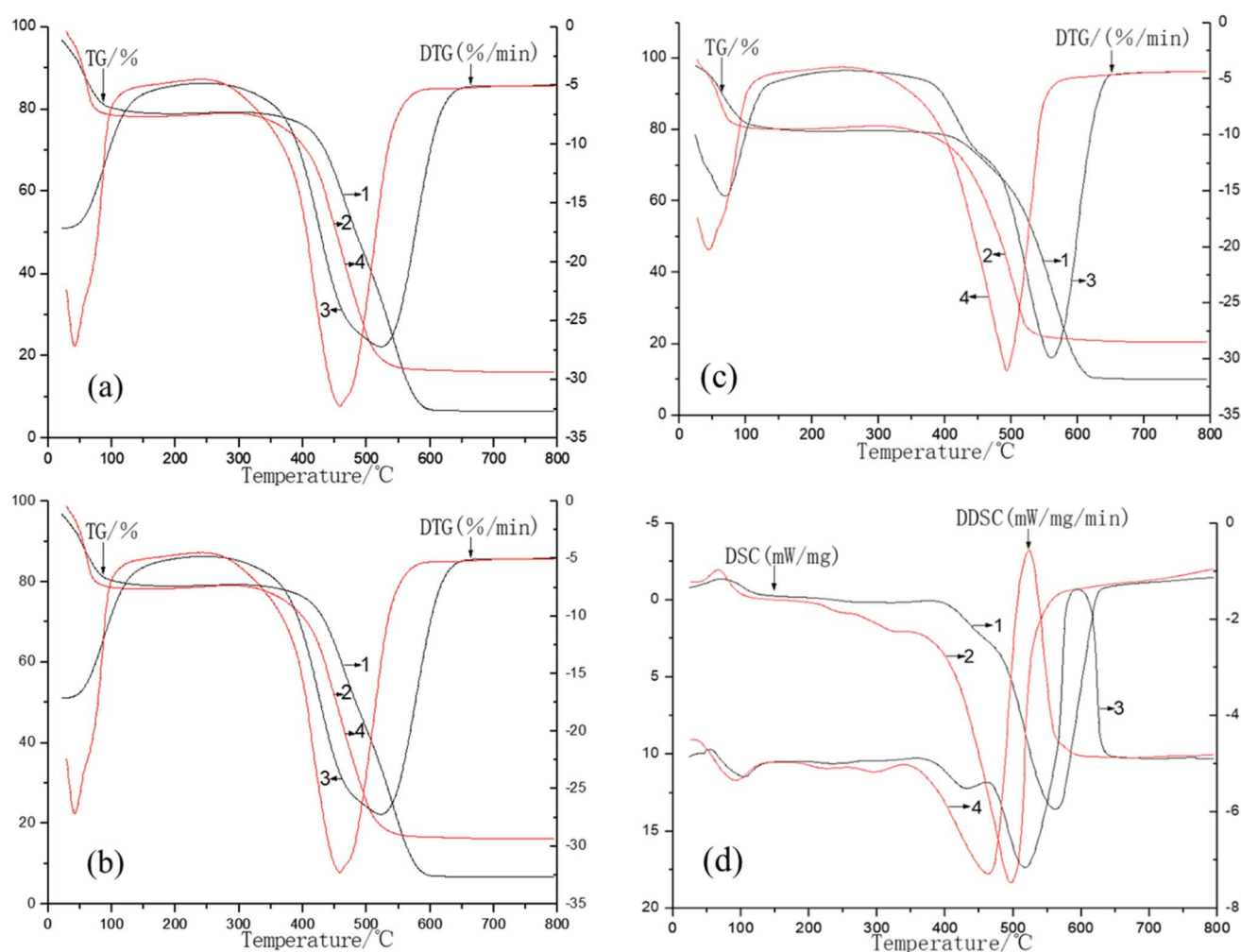

Fig. 8 Raw coal sample under different granularity thermal analysis curves: (a) TG-DTG and (b) DSC-DDSC. Sodium hypophosphite coal samples added under different granularity thermal analysis curves: (c) TG-DTG and (d) DSC-DDSC.
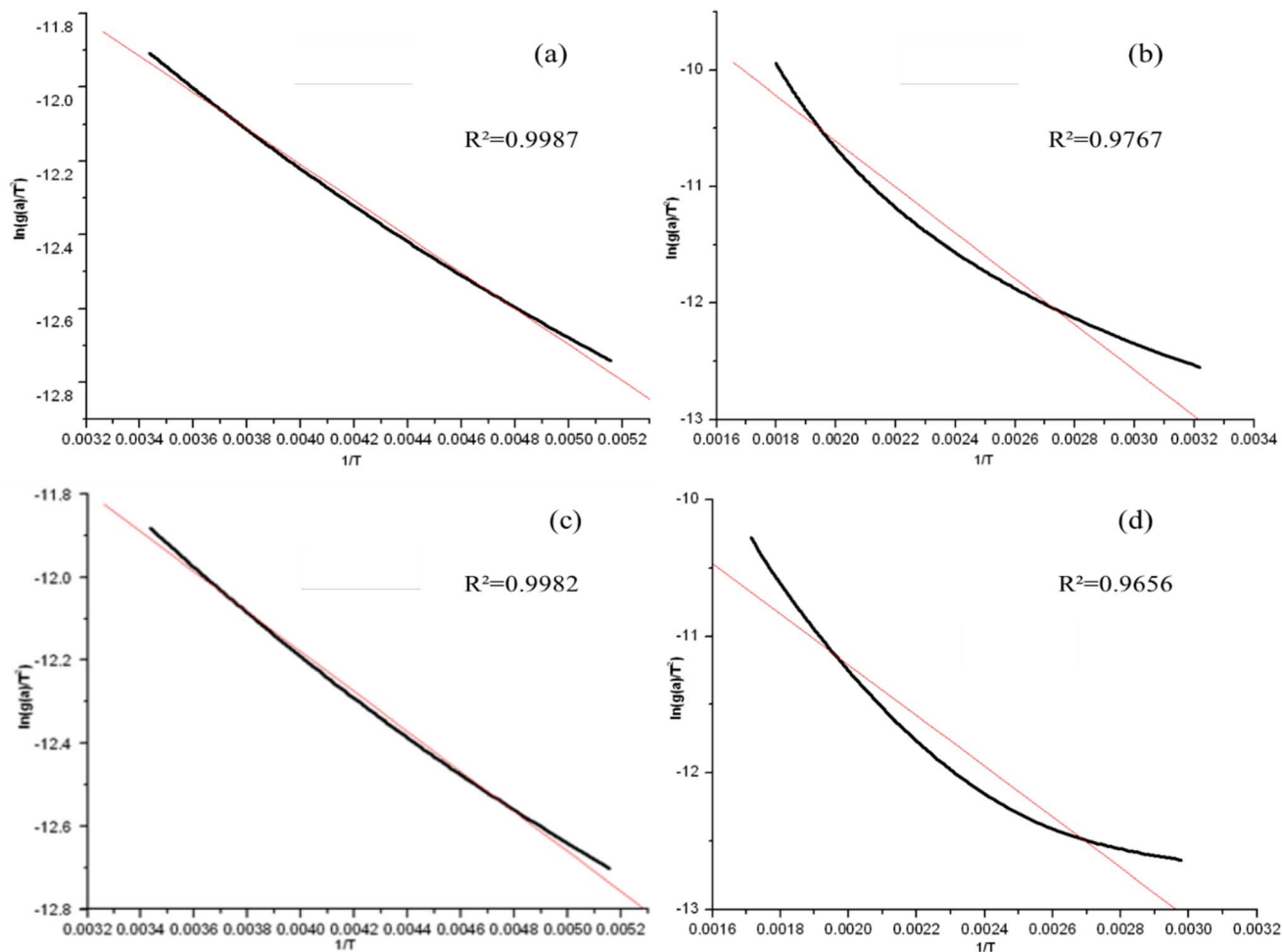
Fig. 9 Coal samples at different stages $\ln\frac{g(\alpha)}{T} - \frac{1}{T}$: (a) oxygen absorption weight gain stage of the raw coal sample; (c) oxygen absorption weight gain stage of the coal sample with added sodium hypophosphite; (b) thermal decomposition stages of the raw coal sample; (d) thermal decomposition stages of the coal sample with added sodium hypophosphite.

mesh coal samples, the maximum heat loss is significantly increased. The main reason is that the increase in coal particle size greatly reduces the specific surface area of coal, resulting in a significant decrease in the contact area between coal and oxygen, reducing the oxidation reaction rate. The inhibitor reacts with the functional groups on the coal surface, further preventing coal oxidation, and the thermogravimetric curve shifts significantly backwards.

3.5 Study on oxidation kinetics performance

After dividing the pyrolysis process of coal into two stages: the initial adsorption weight gain stage and the oxidation weight loss stage, the optimal kinetic mechanism function was found based on the probability mechanism function, and a graph was used to obtain the oxidation pyrolysis kinetic curve of the raw coal sample. The curve was linearly fitted, as shown in Fig. 9, where (a) and (c), respectively, represent the $\ln\frac{g(\alpha)}{T^2}$ to $\frac{1}{T}$ fitting graphs of the oxygen absorption weight gain stage of the raw

coal sample and the coal sample with added sodium hypophosphite, (b) and (d) representing the $\ln\frac{g(\alpha)}{T^2}$ to $\frac{1}{T}$ fitting diagrams of the thermal decomposition stages of the raw coal sample and the coal sample with added sodium hypophosphite, respectively.

From Fig. 9, it can be seen that the activation energy of coal samples varies at different stages of the oxidation process. The activation energy increases continuously with the progress of the reaction. The activation energy of coal samples in the thermal decomposition stage is about twice that of the oxygen absorption weight gain stage. In the initial oxygen absorption weight gain stage, the addition of sodium hypophosphite increases the activation energy of coal samples by 6.72 kJ mol^{-1}[1]. As the reaction continues, the addition of sodium hypophosphite in the thermal decomposition stage increases the activation energy of coal samples by 12.07 kJ mol^{-1}[1] compared to the original coal sample. At this stage, the inhibitory effect of sodium hypophosphite is most significant.

4.   Conclusions

In this work, the addition of sodium hypophosphite as an inhibitor to raw coal was studied to investigate the release of CO during coal oxidation heating process, and the corresponding inhibition rate was calculated. The oxidation inhibition law of coal was analyzed macroscopically.

(1) The best inhibitory effect is achieved with a concentration of 20% sodium hypophosphite, and the higher the temperature, the more favorable the inhibition effect of hypophosphite.

(2) Sodium hypophosphite absorbs water from the surrounding environment during the low-temperature stage, and the intensity of the –OH spectrum peak increases. As the temperature increases, the water evaporates and the spectrum peak gradually decreases. The content of methyl and methylene groups in fatty hydrocarbons is relatively low. With the increase in temperature, the addition of sodium hypophosphite decomposes to produce $H_2PO_2^-$, which combines with H^+ in methyl and methylene to form weak acid hypophosphite. Preventing and delaying the oxidation process of methyl and methylene groups. The structure of $C=C$ in aromatic nuclei is relatively stable, and sodium hypophosphite has a significant early inhibition effect on the RCH_3 and R_2CH_2 groups, and is effective throughout the inhibition of the oxygen-containing functional group C–O.

(3) As the heating rate and coal particle size increase, both the thermal characteristic curve and characteristic temperature show a backward shift. After adding sodium hypophosphite, the maximum heat loss of the coal sample at a heating rate of $10\ ^\circ C\ min^{-1}$ was basically the same as that of the original coal sample. However, the maximum heat loss at a heating rate of $20\ ^\circ C\ min^{-1}$ decreased significantly. The difference in maximum heat loss between the original coal samples at a heating rate of $10\ ^\circ C\ min^{-1}$ and $20\ ^\circ C\ min^{-1}$ was $7.98\ mW\ mg^{-1}$.

(4) After adding sodium hypophosphite, the maximum heat loss of coal samples with a mesh size of 40–80 was not significantly different from that of the original coal sample, but significantly increased compared to coal samples with a mesh size of 150–200 under the same conditions.

(5) The activation energy during the oxidation process of coal samples was calculated, and the addition of sodium hypophosphite increased the activation energy of coal samples by $6.72\ kJ\ mol^{-1}$.

Data availability

All relevant data are within the paper.

Author contributions

Pengjin Liu: investigation; writing–original draft; and writing – review & editing. Hongwei Mu: investigation and project administration. Jiafa Du and Xianwei Dong: funding acquisition; investigation; project administration; writing – original draft; and writing – review & editing. Jianfei Sun: methodology and supervision. Yongliang Zhang: resources and supervision.

Conflicts of interest

The authors declare that there are no potential conflicts of interest in this manuscript.

Acknowledgements

References

1 Z. Jing and H. Wang, Role of an additive in retarding coal oxidation at moderate temperatures, *Proc. Combust. Inst.*, 2011, **33**(2), 2515–2522.

2 R. M. Adar, T. Markovich, A. Levy, *et al.*, Dielectric constant of ionic solutions: combined effects of correlations and excluded volume, *J. Chem. Phys.*, 2018, **149**(5), 54504.

3 Z. Baolong, Technical research on reducing the spontaneous combustion of coal waste dump through hierarchical pretreatment, *Appl Energy Technol.*, 2022, (3), 1–4.

4 F. W. Dai, Quantum chemical application in inhibitor suppressed the spontaneous combustion of coal, *Adv. Mater. Res.*, 2012, **524–527**, 658–661.

5 Z. Mrabet, M. Alsamara, A. S. Saleh and S. Anwar, Urbanization and non-renewable energy demand: a comparison of developed and emerging countries, *Energy*, 2019, **170**, 832–839.

6 N. Wang, R. Shen, Z. Wen and D. D. Clercq, Life cycle energy efficiency evaluation for coal development and utilization, *Energy*, 2019, **179**, 1–11.

7 Z. Song and C. Kuenzer, Coal fires in China over the last decade: a comprehensive review, *Int. J. Coal Geol.*, 2014, **133**, 72–99.

8 J. Xu, W. Gao, H. Xie, J. Dai, C. Lv, M. Li, *et al.*, Integrated tech-paradigm based innovative approach towards ecological coal mining, *Energy*, 2018, **151**, 297–308.

9 J. Deng, Y. Xiao, Q. Li, J. Lu and H. Wen, Experimental studies of spontaneous combustion and anaerobic cooling of coal, *Fuel*, 2015, **157**, 261–269.

10 J. Pandey, N. K. Mohalik, R. K. Mishra, A. Khalkho and D. Kumar, Investigation of the role of fire retardants in preventing spontaneous heating of coal and controlling coal mine fires, *Fire Technol.*, 2015, **51**, 227–245.

11 X. Qi, D. Wang, H. Xin and G. Qi, An in situ testing method for analyzing the changes of active groups in coal oxidation at low temperatures, *Spectrosc. Lett.*, 2014, **47**, 495–503.

12 Z. Li, B. Kong, A. Wei, Y. Yang and Y. Zhou, Free radical reaction characteristics of coal low-temperature oxidation

and its inhibition method, *Environ. Sci. Pollut. Res.*, 2016, **23**, 593–605.

13 R. D. Rogers and K. R. Seddon, Ionic liquids-solvents of the future?, *Science*, 2003, **302**, 792–793.

14 L. Wang, Y. Xu, S. Jiang, M. Yu, T. Chu, W. Zhang, *et al.*, Imidazolium based ionic liquids affecting functional groups and oxidation properties of bituminous coal, *Saf. Sci.*, 2012, **50**, 1528–1534.

15 Y. Xiao, Q. W. Li, J. Deng, C. M. Shu and W. Wang, Experimental study on the corresponding relationship between the index gases and critical temperature for coal spontaneous combustion, *J. Therm. Anal. Calorim.*, 2017, **127**, 1009–1017.

16 A. Ponzio, S. Senthoorselvan, W. Yang, W. Blasiak and O. Eriksson, Ignition of single coal particles in high-temperature oxidizers with various oxygen concentrations, *Fuel*, 2008, **87**, 974–987.

17 Y. Xiao, S. J. Ren, J. Deng and C. M. Shu, Comparative analysis of thermokinetic behavior and gaseous products between first and second coal spontaneous combustion, *Fuel*, 2018, **227**, 325–333.

18 A. Tahmasebi, J. Yu, H. Su, Y. Han, J. Lucas, H. Zheng, *et al.*, A differential scanning calorimetric study on the characteristics and behavior of water in low-rank coals, *Fuel*, 2014, **135**(11), 243–252.

19 J. Deng, J. Zhao, Y. Zhang, A. Huang, X. Liu, X. Zhai, *et al.*, Thermal analysis of spontaneous combustion behavior of partially oxidized coal, *Process Saf. Environ. Prot.*, 2016, **104**, 218–224.

20 J. Deng, J. Zhao, A. Huang, Y. Zhang, C. Wang and C. Shu, Thermal behavior and microcharacterization analysis of second-oxidized coal, *J. Therm. Anal. Calorim.*, 2017, **127**, 439–448.

21 J. Deng, Y. Xiao, Q. Li, J. Lu and H. Wen, Experimental studies of spontaneous combustion and anaerobic cooling of coal, *Fuel*, 2015, **157**, 261–269.

22 A. González-Cencerrado, B. Peña and A. Gil, Coal flame characterization by means of digital image processing in a semi-industrial scale PF swirl burner, *Appl. Energy*, 2012, **94**, 375–384.

23 S. Dai, D. Ren, Ch-K. Chou, R. Finkelman, V. Serendin and Y. Zhou, Geochemistry of trace elements in Chinese coals: a review of abundances genetic types, impacts on human health and industrial utilization, *Int. J. Coal Geol.*, 2012, **94**, 3–21.

24 J.-F. Sun, Yu-J. Qin, Y.-L. Zhang, Z.-Y. Sa, J. Liu, Yu-H. Wang, C.-Y. Wang a and Q.-L. Tan, Homogeneous and heterogeneous ionic liquids catalyze CO_2 cycloaddition reaction, *J. Mol. Struct.*, 2025, **1322**, 140534.

25 J.-F. Sun, Y.-L. Zhang, Z.-Y. Sa, J. Liu, D.-Y. Liu, C.-Y. Tian, Q.-L. Tan and N. Wang, Kinetic modeling, optimization and guidance of a Novel ionic liquid membrane reactor for Enhanced mass transfer processes in CO_2 cycloaddition reactions, *Chem. Eng. J.*, 2025, **505**, 159599.

26 A. C. Smith, Y. Miron and C. P. Lazzara, *Inhibition of Spontaneous Combustion of Coal*, US Bureau of Mines, 1988.

27 Y. Adachi and H. Sugawara, Inhibitor for Inhibiting Carbonaceous Powder from Heating up/spontaneously Igniting, *US Pat.* 0069149, 2003.

28 J. Li, Z. Li, Y. Yang, *et al.*, Laboratory study on the inhibitory effect of free radical scavenger on coal spontaneous combustion, *Fuel Process. Technol.*, 2018, **171**, 350–360.

29 ISO 18283: 2006, *Method for Preparation of Coal Sample, Hard Coal and coke-Manual Sampling*, MOD, GB474-2008.

30 ISO D21, *Determination of carbon and hydrogen in coal. GB/T 476-2008 We will add the above key information to the manuscript*, 2008.

31 M. Zhu, Experimental research of spontaneous combustion suppression with inhibitors in Yangquan No. 5 coal mine $15^{\#}$ coal seam, *Coal Eng.*, 2016, **48**(4), 93–95, DOI: **10.11799/ce201604028**.

32 W. Lu, H. Qian-Ting, X. Zhong and D. Wang, Gradual self-activation reaction theory of spontaneous combustion of coal, *J. China Univ. Min. Technol.*, 2007, **36**(1), 110–113.

33 Z. Lan-fang, Test and Analysis on Salty retardants performance to restrain coal oxidized spontaneous combustion, *Coal Sci. Technol.*, 2010, **38**(5), 70–73.

34 L. Yao, F. Wang, X. Dong, *et al.*, Study on the characteristics and microscopic mechanism of coal spontaneouscombustion based on programmed heating experiment, *Coal Sci. Technol.*, 2024, **52**(S1), 94–106.

35 H.-F. Lü, Y. Xiao, J. Deng, D. Li, L. Yin and C.-M. Shu, Inhibiting effects of 1-butyl-3-methyl imidazole tetrafluoroborate on coal spontaneous combustion under different oxygen concentrations, *Energy*, 2019, **186**, 115907.

36 S. B. Singh and S. A. Dastghei, Characteristics of graphene oxide-like materials prepared from different deashed-devolatilized coal chars and comparison with graphite-based graphene oxide, with or without the ultrasonication treatment, *Carbon*, 2024, **228**, 119331.

37 S. B. Singh, N. Haskin and S. A. Dastghei, Coal-based graphene oxide-like materials: a comprehensive review, *Carbon*, 2023, **215**, 118447.

38 H. Takagi, K. Maruyama, N. Yoshizawa, Y. Yamada and Y. Sat, XRD analysis of carbon stacking structure in coal during heat treatment, *Fuel*, 2004, **83**(17–18), 2427–2433.

39 H. F. Lü, Experimental research on the thermal effect and kinetics of imidazolium ionic liquids for inhibiting coal spontaneous combustion, Master thesis, Xian University of Science and Technology, Shaanxi Province, PR China, 2017.

40 H. H. Wang, B. Z. Dlugogorski and E. M. Kennedy, Coal oxidation at low temperatures: oxygen consumption, oxidation products, reaction mechanism and kinetic modelling, *Prog. Energy Combust.*, 2003, **29**, 487–513.

41 J. Cummings, P. Tremain, K. Shah, E. Heldt, B. Moghtaderi, R. Atkin, *et al.*, Modification of lignites via low temperature ionic liquid treatment, *Fuel Process. Technol.*, 2016, **155**, 51–58.

42 J. Chen, X. Li, Y. Fu, *et al.*, A study on co-combustion reaction performance of rape straw and lignite, *J. Inn. Mong. Univ. Technol. (Nat. Sci. Ed.)*, 2024, **43**(06), 535–541.